Supplementary information for

Xiaoyuan Wang, Meng Li, Rong Cheng, Liting Zhao, Yanfeng Xi, Jianming Wang, Peng Gao, Lingqian Chang, Zixian Liu, Di Huang, Shengbo Sang, 2025. Nuclear-targeted reactive oxygen species storm: a self-amplifying nanoplatform that overcomes hypoxia and redox barriers for enhanced sonodynamic cancer therapy. *Bio-Des Manuf*, 8(5):776-799. https://doi.org/10.1631/bdm.2500021

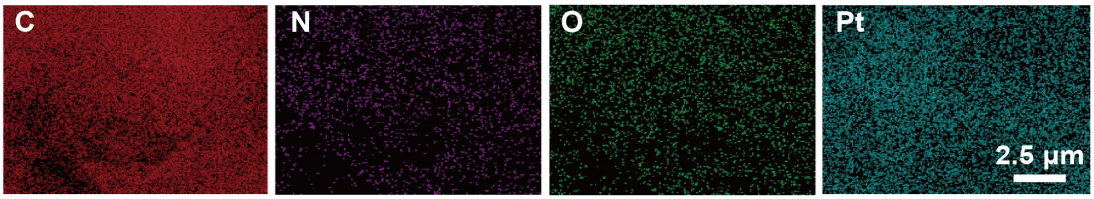


Fig. S1 Elemental distribution mapping images of Pt^{2+}-CDs@PpIX, including carbon (C), nitrogen (N), oxygen (O), and platinum (Pt)

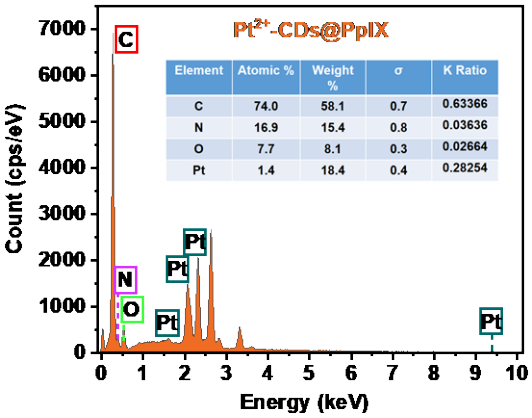


Fig. S2 EDS spectrum of Pt^{2+}-CDs@PpIX

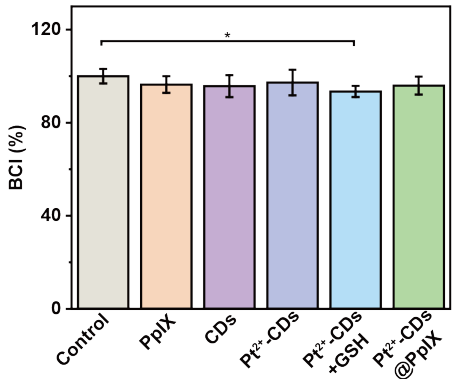


Fig. S3 The coagulation index of different materials, $^{*}p<0.05$

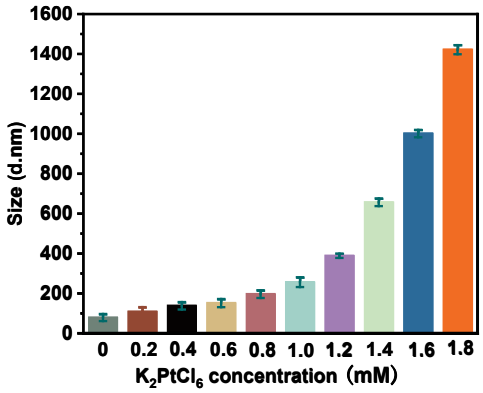


Fig S4 Hydrodynamic diameters of Pt^{2+}-CDs prepared by adding different concentrations of K_2PtCl_6 to CDs (1 μM)

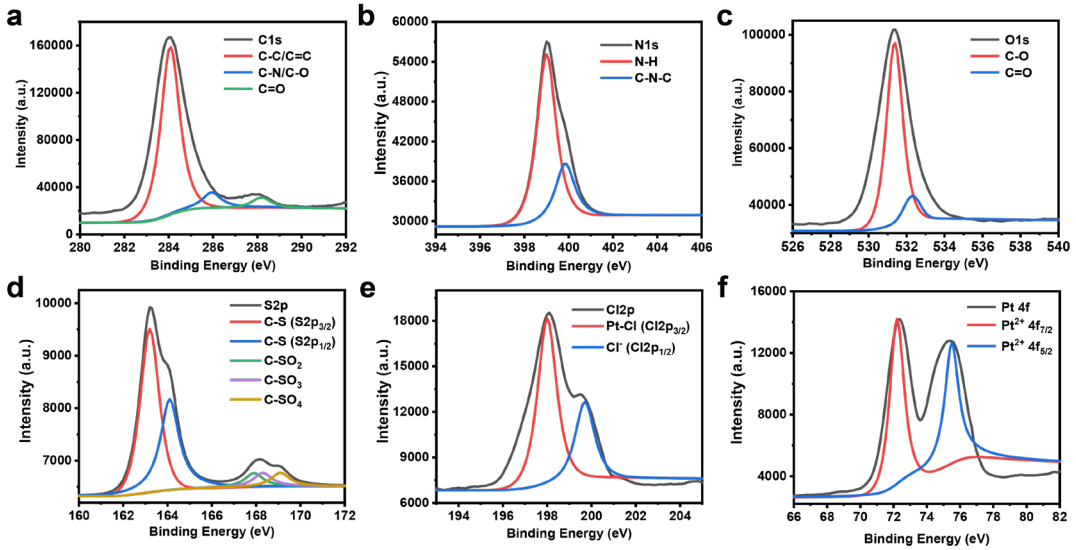


Fig. S5 High-resolution C 1s (a), N 1s (b), O 1s (c), S 2p (d), Cl 2p (e), and Pt 4f (f) XPS spectra of Pt^{2+}-CDs@PpIX

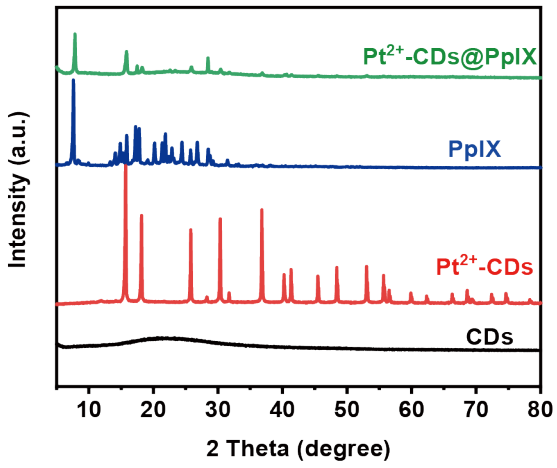


Fig. S6 XRD pattern of CDs, Pt^{2+}-CDs, PpIX, and Pt^{2+}-CDs@PpIX

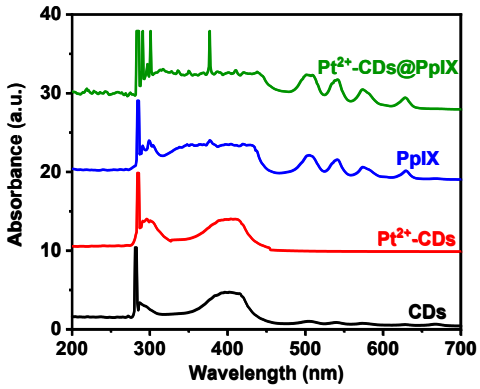


Fig. S7 UV absorption spectra of CDs, Pt^{2+}-CDs, PpIX, and Pt^{2+}-CDs@PpIX

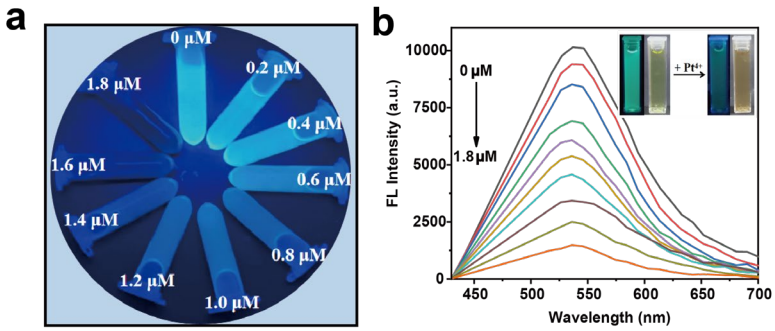


Fig. S8 (a) The fluorescence quenching diagram after adding different concentrations of Pt^{4+} into CDs. (b) Fluorescence spectra of CDs solutions (60 μg/mL, pH=7) added with various concentrations of Pt^{4+}

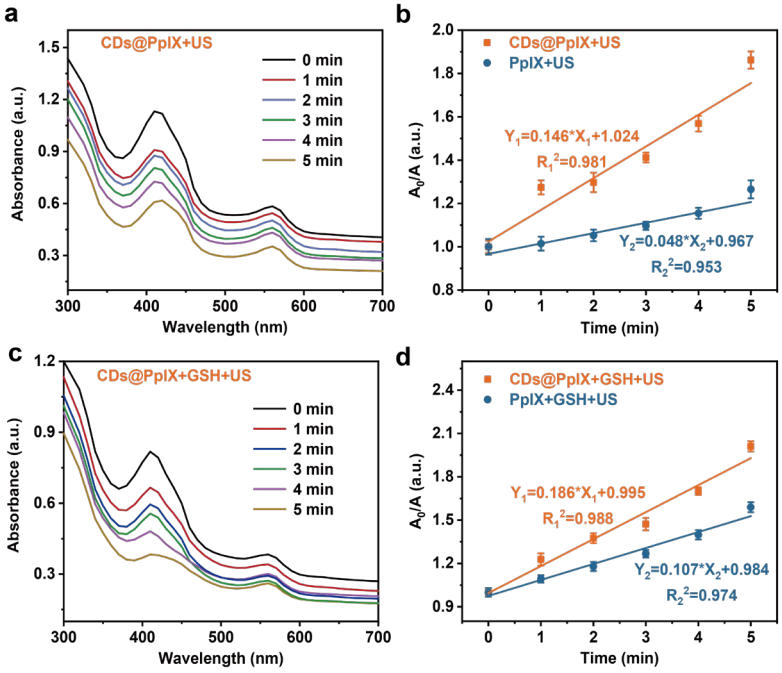


Fig. S9 Time-dependent 'O2 generation by CDs@PpIX (a) and CDs@PpIX+GSH (c) under US irradiation. The rate constant of 'O2 generation in the presence of CDs@PpIX, PpIX (b) and CDs@PpIX+GSH, PpIX+GSH (d) under US irradiation

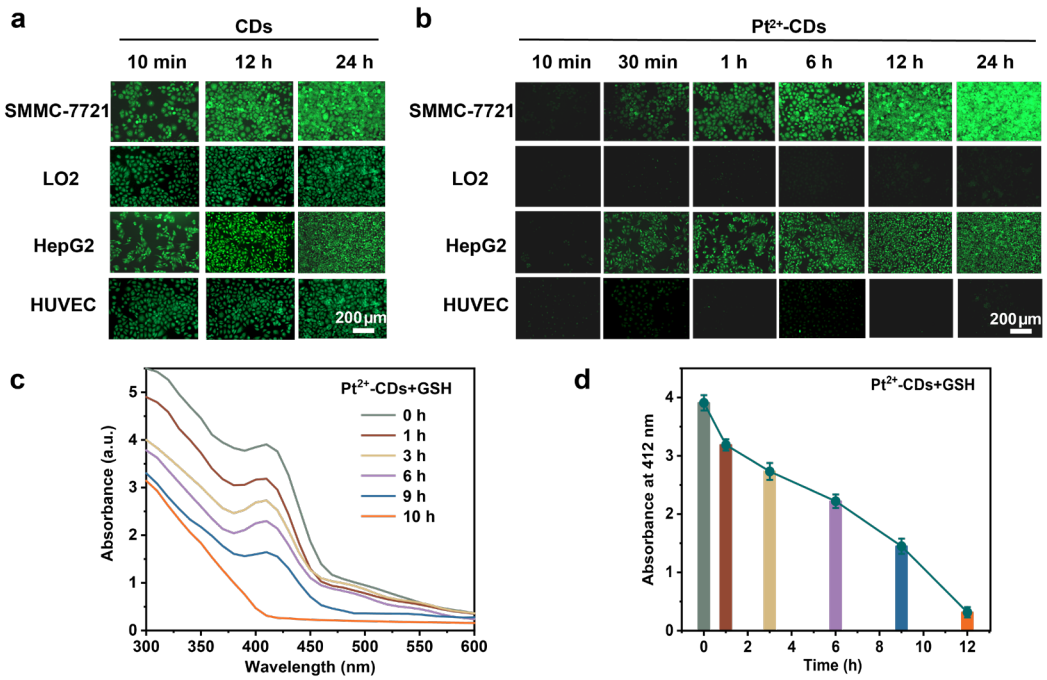


Fig. S10 Fluorescence images of SMMC-7721, LO2, HepG2, and HUVEC cells treated with CDs (a), Pt^{2+}-CDs (b) for different times. Time-dependent GSH depletion by Pt^{2+}-CDs using DTNB as the GSH indicator (c, d)

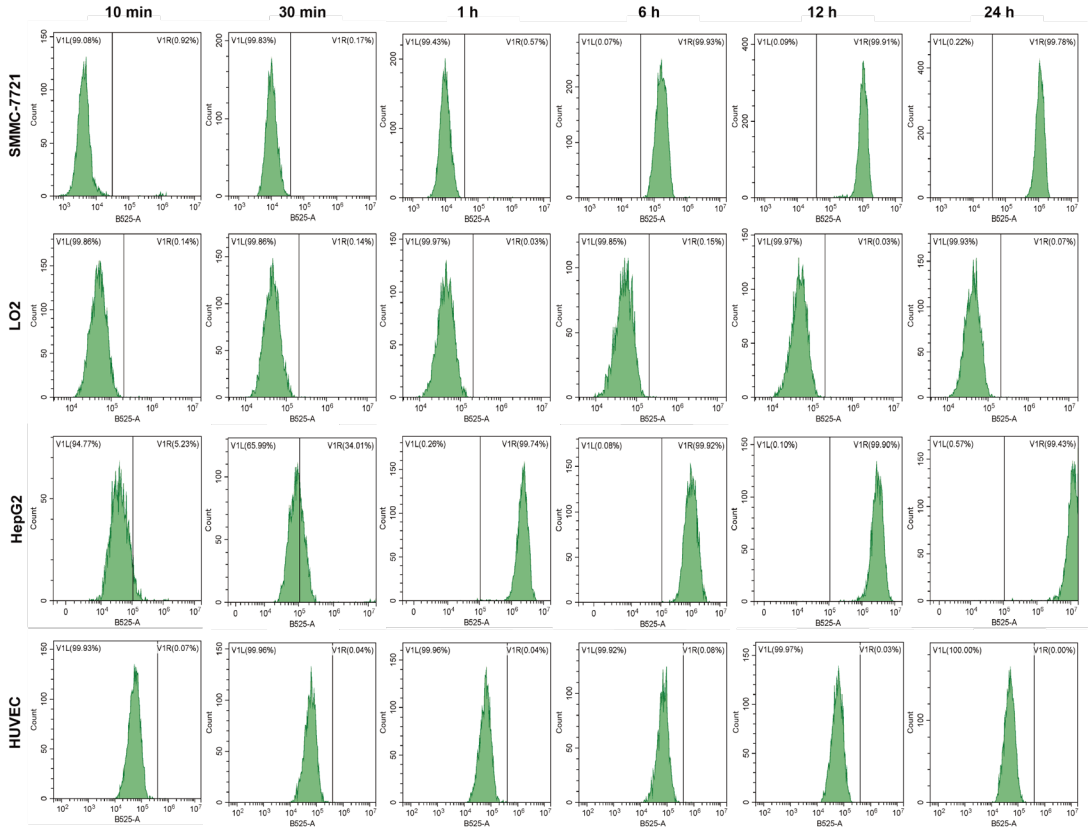


Fig. S11 Flow cytometry of SMMC-7721, LO2, HepG2, and HUVEC cells treated with Pt^{2+}-CDs@PpIX for different times

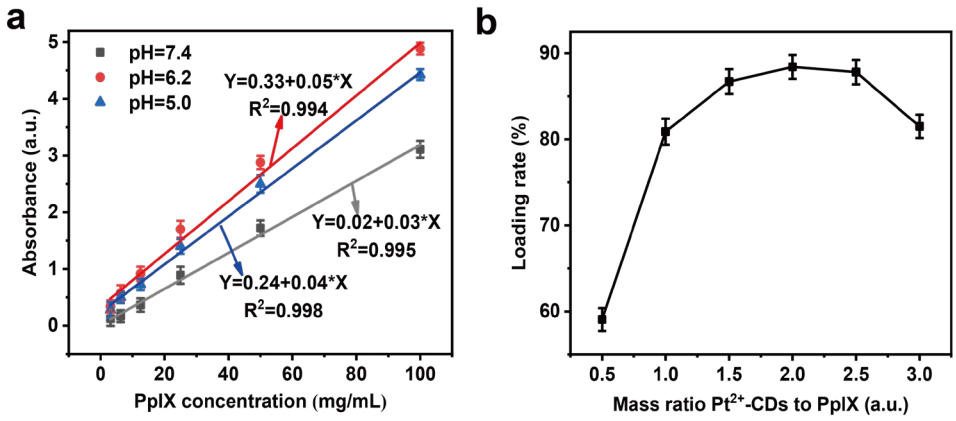


Fig. S12 (a) Standard curves of PpIX concentration versus absorbance in DMSO solution with different pH values. (b) Loading rates for different mass ratios of Pt^{2+}-CDs to PpIX

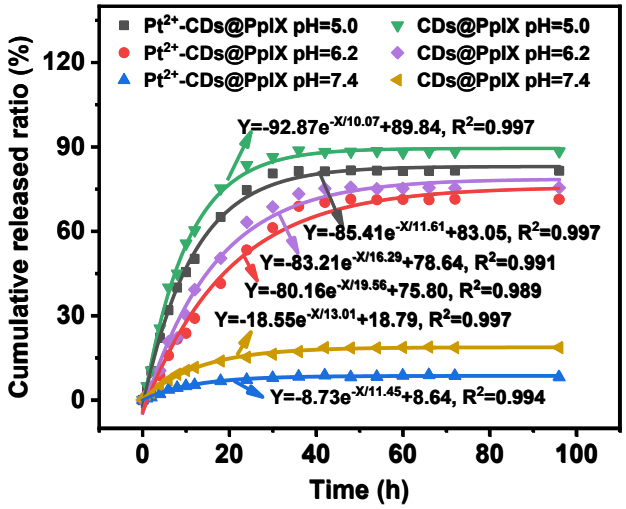


Fig. S13 In vitro release profiles of CDs@PpIX and Pt^{2+}-CDs@PpIX

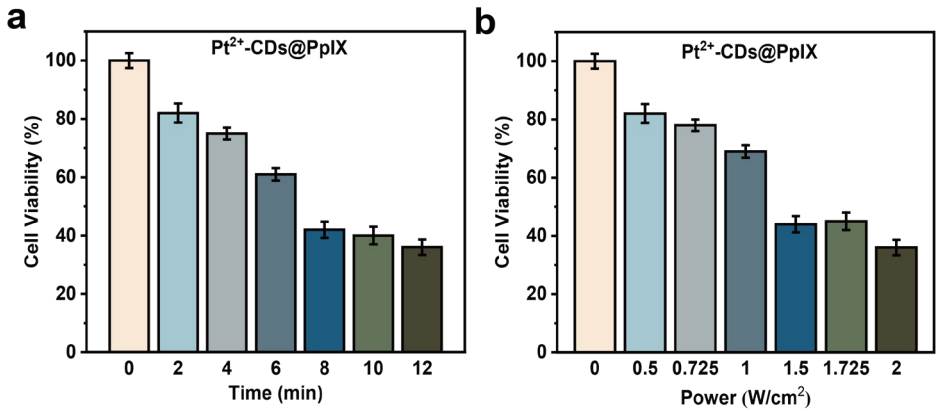


Fig. S14 (a) Cell viability of SMMC-7721 cells exposed to different ultrasound times. (b) Cell viability of SMMC-7721 cells exposed to different ultrasound intensities

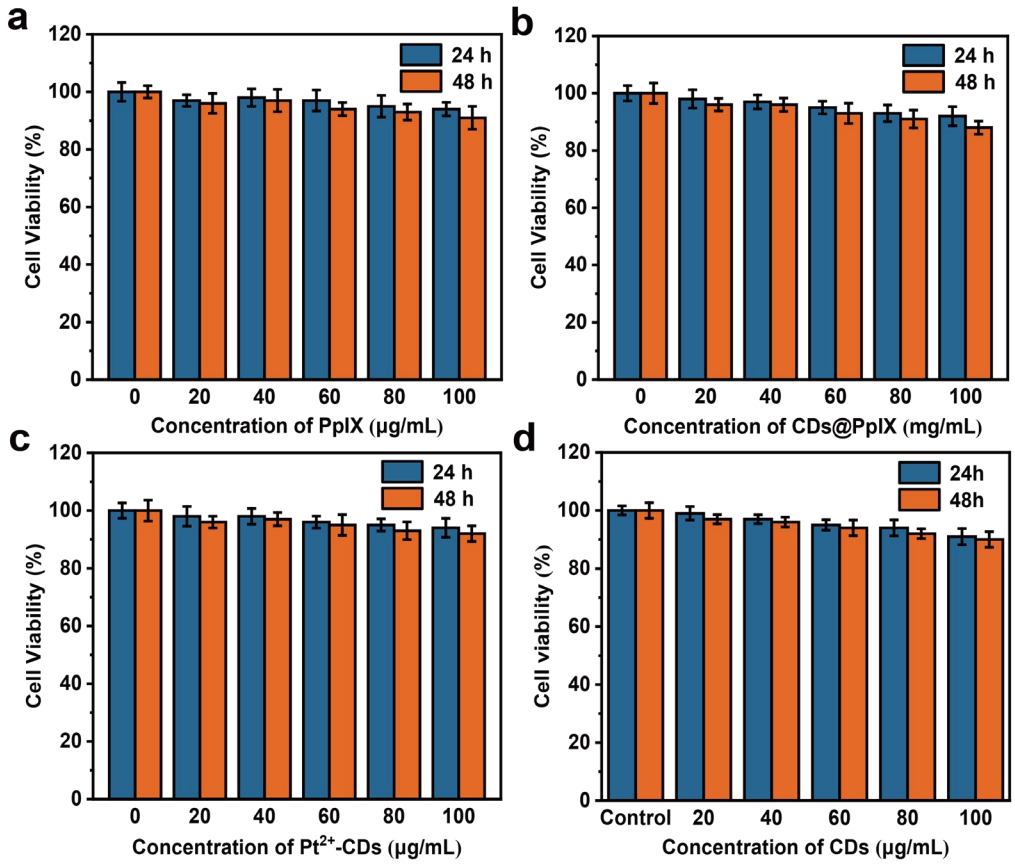


Fig. S15 Relative cell viability after incubation of SMMC-7721 cells with different concentrations of PpIX (a), CDs@PpIX (b), Pt^{2+}-CDs (c), and CDs (d)

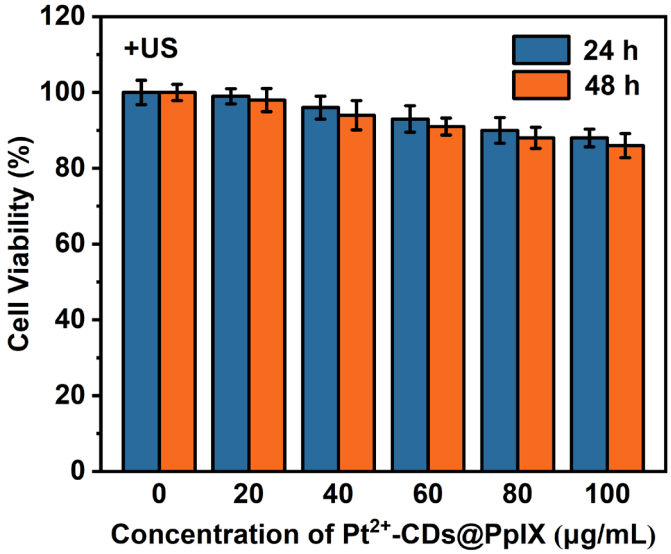


Fig. S16 Relative cell viability after incubation of LO2 cells with different concentrations of Pt^{2+}-CDs@PpIX

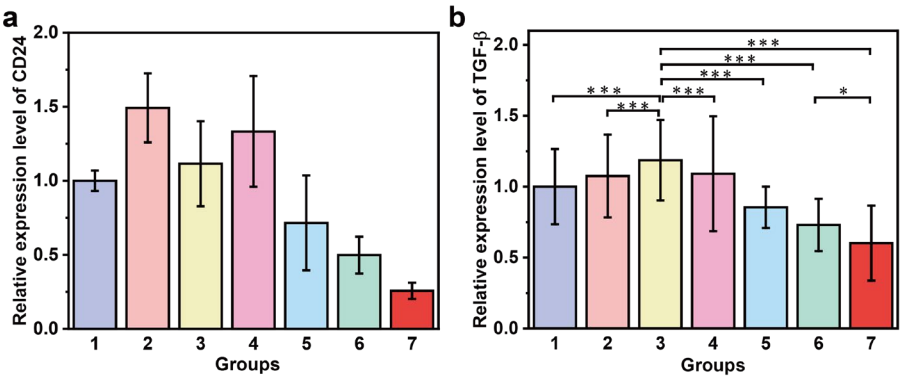


Fig. S17 The mRNA expression of the associated proteins was observed on the SMMC-7721 cells in the 3DM-7721 model by different treatments. Group 1: Control; Group 2: US; Group 3: Pt^{2+}-CDs@PpIX; Group 4: Pt^{2+}-CDs+US; Group 5: PpIX+US; Group 6: CDs@PpIX+US; Group 7: Pt^{2+}-CDs@PpIX+US

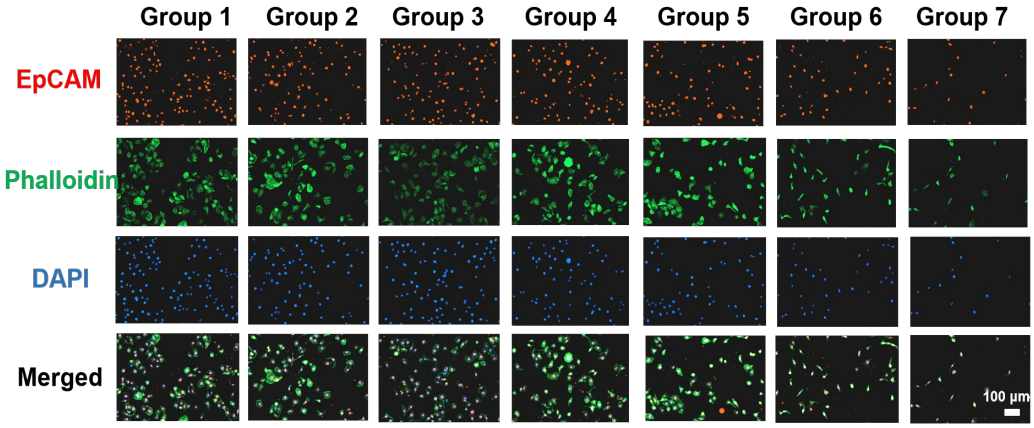


Fig. S18 Immunofluorescence staining of SMMC-7721 cells after treatment with different drugs for EpCAM. Group 1: Control; Group 2: US; Group 3: Pt^{2+}-CDs@PpIX; Group 4: Pt^{2+}-CDs+US; Group 5: PpIX+US; Group 6: CDs@PpIX+US; Group 7: Pt^{2+}-CDs@PpIX+US

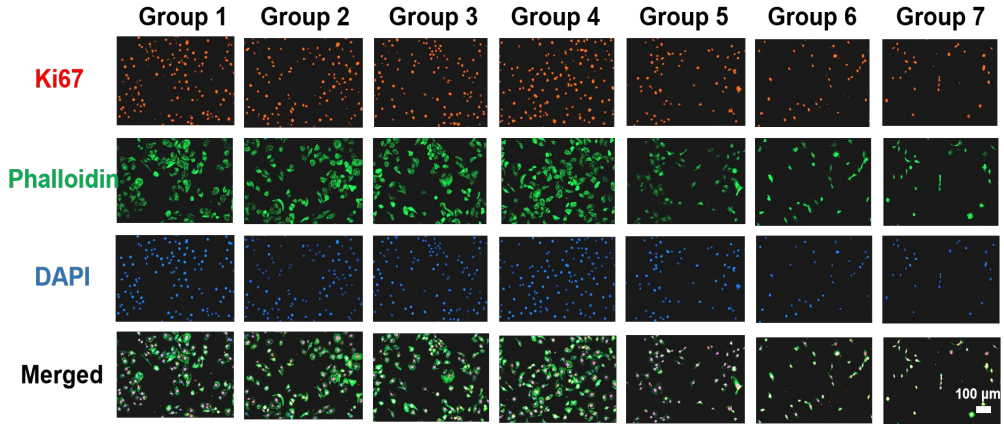


Fig. S19 Immunofluorescence staining of SMMC-7721 cells after treatment with different drugs for Ki67. Group 1: Control; Group 2: US; Group 3: Pt^{2+}-CDs@PpIX; Group 4: Pt^{2+}-CDs+US; Group 5: PpIX+US; Group 6: CDs@PpIX+US; Group 7: Pt^{2+}-CDs@PpIX+US

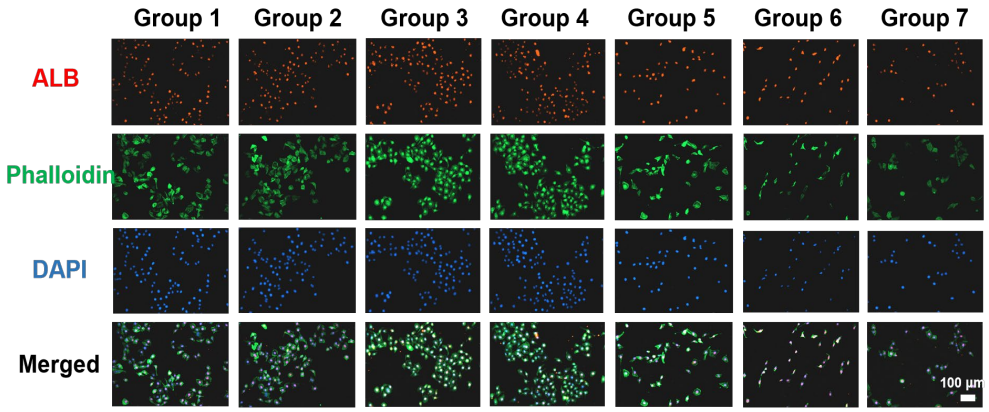


Fig. S20 Immunofluorescence staining of SMMC-7721 cells after treatment with different drugs for ALB. Group 1: Control; Group 2: US; Group 3: Pt^{2+}-CDs@PpIX; Group 4: Pt^{2+}-CDs+US; Group 5: PpIX+US; Group 6: CDs@PpIX+US; Group 7: Pt^{2+}-CDs@PpIX+US

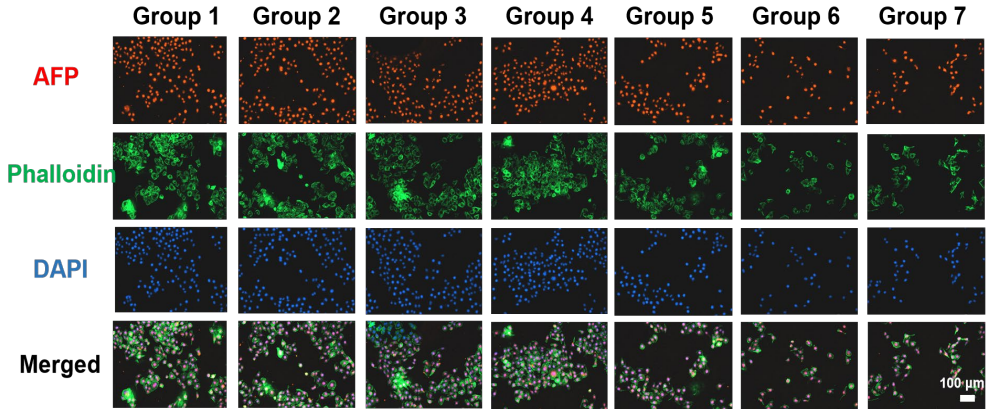


Fig. S21 Immunofluorescence staining of SMMC-7721 cells after treatment with different drugs for AFP. Group 1: Control; Group 2: US; Group 3: Pt^{2+}-CDs@PpIX; Group 4: Pt^{2+}-CDs+US; Group 5: PpIX+US; Group 6: CDs@PpIX+US; Group 7: Pt^{2+}-CDs@PpIX+US

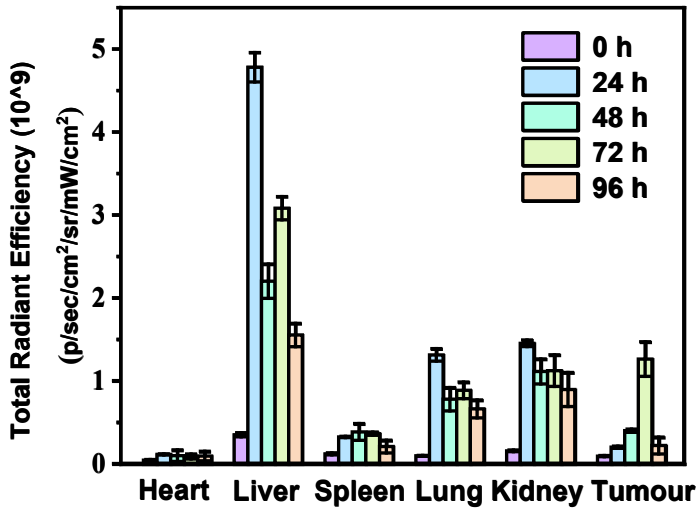


Fig. S22 The corresponding relative fluorescence intensity of major organs and tumors of sacrificed mice was shown in Fig. 8c

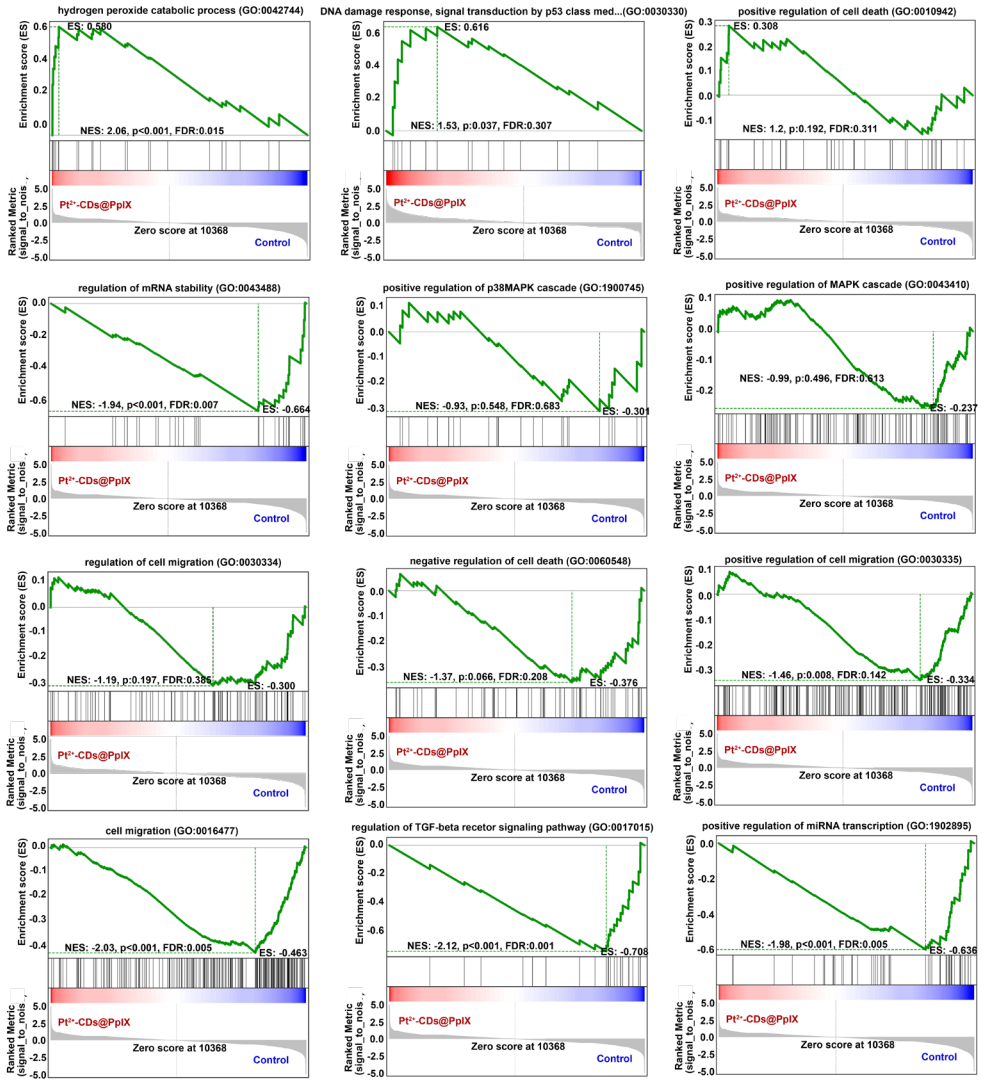


Fig. S23 Gene set enrichment analysis (GSEA) of RNA-seq data for Pt^{2+}-CDs@PpIX vs. Control

Table S1 The antibodies for immunofluorescent

Antibodies	Concentration	Source
Anti-EPCAM Antibody	1:100	Abcam
AFP Rabbit pAb	1:250	Abcam
ALB Rabbit pAb	1:100	Abcam
Ki67 Rabbit pAb	1:200	Abcam
Anti-Oxoguanine 8 Antibody	1:200	Abcam
Anti-53BP1 Antibody	1:200	Abcam
Goat Anti-rabbit IgG (H+L)	1:500	Abcam

Table S2 The primers for qPCR

Gene	Forward (5′-3′)	Reverse (5′-3′)
Ki67	AACTATGGAACTGGGATGGAGAGG	AGTGTGGTCTGGTGTCTGGAAG
AFP	AAATTT TGGGACCCGAACTTTC	ACAGAGTGTCTTGAGAACA
CD133	TCTGGGTCTACAAGGACTTTCC	GCCCGCCTGAGTCACTAC
EpCAM	AATCGTCAATGCCAGTGTACT T	TCTCATCGCAGTCAGGATCATAA
TGF-β	GCAACAATTCCTGGCGATACCTC	CCTCCACGGCTCAACCACTG
CD24	TTCTCCAAGCACCCAGCA	TGGAATAAATCTGCGTGGGTA
Bcl-2	CGAGTGGGATGCGGGAGATG	CGGGATGCGGCTGGATGG
53BP1	GGCTGTCTGATGTGGATGCTAATAC	CTTGCTGGACTGTTCTGCTATGG
β-actin	GAGCTGCGTGTGGCTCCC	CCAGAGGCGTACAGGGATAGCA

Table S3 The antibodies for western blot

Antibodies	Concentration	Source
GAPDH	1:1000	Boster
p53	1:1000	Boster
BAX	1:1000	Boster
Bcl-2	1:1000	Boster

Table S4 The antibodies for immunohistochemistry

Antibodies	Concentration	Source
CD31/PECAM1 Rabbit pAb	1:400	Abcam
Ki67 Rabbit pAb	1:400	Abcam